

# The effects of scintillations on the positioning errors

Yannick Béniguel<sup>(1)</sup>, J. Geiswiler<sup>(1)</sup>, J-P Adam<sup>(1)</sup>, Christophe Sarrou<sup>(2)</sup>, Christophe Sajous<sup>(2)</sup>, Thibault De Maeyer<sup>(2)</sup>

(1) IEEA, Courbevoie, France

(2) DGA/LRBA, Vernon, France

**Abstract :** This paper deals with the problem of ionosphere scintillations and their impact on the GPS positioning errors

## 1. Introduction

This paper deals with the problem of the scintillations on GPS satellites links and their effect on the positioning error. These scintillations result from propagation through the ionosphere inside which inhomogeneities have developed and create random variations of the medium index. These inhomogeneities create a number of modifications on the signals, among them phase and intensity fluctuations, fluctuations of the arrival angle, dispersivity, Doppler... The ionosphere scintillations are especially important at equatorial and auroral regions. Equatorial scintillations appear after sunset and may last a few hours. They are related in particular to the solar activity and the season.

In this paper we consider two things :

- How to estimate and characterize the scintillations
- How to implement the corresponding signal in a simulator in order to reproduce the links characteristics and to estimate the positioning error

To estimate and characterize the scintillations is done using the GISM model developed at IEEA. GISM uses the Multiple Phase Screen technique (MPS). It consists in a resolution of the parabolic equation (PE) for a medium divided into successive layers, each of them acting as a phase screen. It provides the statistical characteristics of the transmitted signals, in particular the scintillation index, the fade durations and the

cumulative probability of the signal consequently allowing determination of the margins to be included in a budget link.

The phase noise at receiver level is composed of three terms, the most significant being the thermal noise which is directly related to the scintillations index. The way it affects the Delay Lock Loop (DLL) is detailed in this paper. The fluctuations of intensity decrease the signal to noise ratio and are considered concurrently. This calculation is derived here together with the probability of loss of lock and the positioning error.

An extension of the model has been developed as a random generator producing time series with the corresponding statistical properties (s4 and related spectrum) allowing assessing the capability of a receiver to resist to scintillations. The way this generator is included in a global GPS / Glonass simulator is presented in this paper.

## 2. GISM Propagation Model

### 2.1 Medium modeling

The electronic density inside the medium is calculated by the NeQuick model developed by Universities of Graz and Trieste. Inputs of this model are the solar flux number, the year, the day of the year and the local time. It provides the electronic density average value for any point in the ionosphere (latitude, longitude, altitude). NeQuick model is used as a subroutine in the GIM model.

## 2.2 Algorithm

Propagation errors are of two kinds :

- Mean errors,
- Scintillations and more generally higher order moments of the signal.

Mean errors are obtained solving the ray equation. The ray differential equation is solved by Runge Kutta algorithm. The line of sight is defined taking the electron density gradient at each point along the ray into account. This is done with respect to the three axes in a geodesic referential system. This is an iterative algorithm. It is stopped when the ray crosses the plane perpendicular to the line of sight and containing the source point. The mean errors : range, angular and Faraday rotation are subsequently determined.

The calculation of fluctuations is a 2D calculation. The first dimension  $z$  is the line of sight previously determined. The second dimension  $x$  is perpendicular to this. Since the problem is solved as a two-dimensional one, the medium of propagation is considered to be homogeneous in the third direction, which is perpendicular to the first two directions. The propagation of the monochromatic component of the field  $E$  in the random medium is described by Helmholtz equation

$$\nabla^2 E + k^2(z)[1 + \varepsilon(x, z)]E = 0, \quad (1)$$

where  $k^2(z) = \omega^2 \varepsilon_0(z)/c^2$  is the local wave number,  $\varepsilon_0(z)$  is the background dielectric permittivity along the main propagation axis  $z$ ,  $\varepsilon(x, z)$  is the random field of the relative dielectric permittivity.

Introducing the complex amplitude  $U(x, z)$  of the stochastic field

$$E(x, z) = U(x, z) \exp\left(i \int_0^z k(z) dz\right), \quad (2)$$

and assuming that the variation of the complex amplitude is mainly in the direction perpendicular to the main propagation axis

(parabolic approximation), the stochastic parabolic equation for the complex amplitude can be written in the form:

$$2ik \frac{\partial U}{\partial z} + \nabla_t^2 U + k^2 \varepsilon U = 0, \quad (3)$$

where  $\nabla_t^2$  is the transversal Laplacian.

To solve equation (3), the medium is divided into series of successive layers perpendicular to the main propagation axis, each one being characterized by local homogeneous statistical properties. The solution is then obtained by iterating successively scattering and propagation calculations as detailed hereafter. The parabolic wave equation (3) is split into two equations. The first one describes the phase change due to the presence of random fluctuations  $\varepsilon(x, z)$

$$2ik \frac{\partial U}{\partial z} + k^2 \varepsilon U = 0, \quad (4)$$

and the second equation describes propagation in the space without fluctuations

$$2ik \frac{\partial U}{\partial z} + \nabla_t^2 U = 0. \quad (5)$$

Introducing the small step  $\Delta z$  along the main propagation axis, the solution of the successive couple of equations (4,5) can be obtained in the form

$$U(x, z + \Delta z) = \left(\frac{k}{2i\pi\Delta z}\right)^{1/2} \int U(x', z) \exp\left(\frac{ik\Delta z}{2} \varepsilon(x', z)\right) \exp\left(\frac{ik(x-x')^2}{2\Delta z}\right) dx'$$

In equation (6) above, the first exponent under the integral sign arises from the solution to the equation (4), and the second exponent together with the factor before the integral sign is the Green's function for the equation (5). In practice the convolution integral (6) is calculated by means of fast Fourier transformation. Applying equation (6) to each layer, the solution to the parabolic equation (3) is obtained. This technique is referred in the literature as multiple phase screen technique.

### Random medium synthesis

The spectral density of the phase at the output of the medium is written as the product of the Fourier transform of a centered gaussian random variable by the square root of the spectral density of the signal that we want to synthesize. The resulting random variable meets the required conditions. The corresponding signal is obtained taking the inverse Fourier transform of this product.

### Results obtained

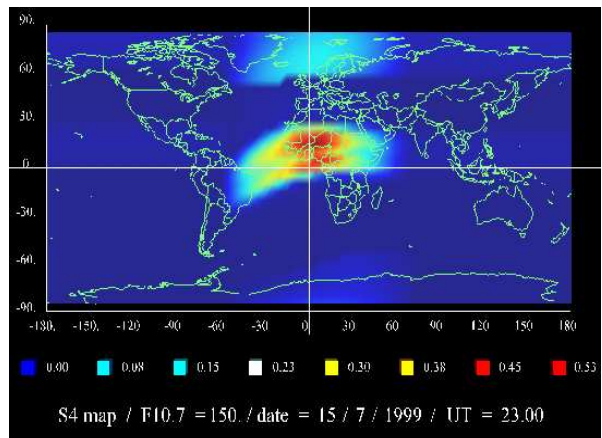
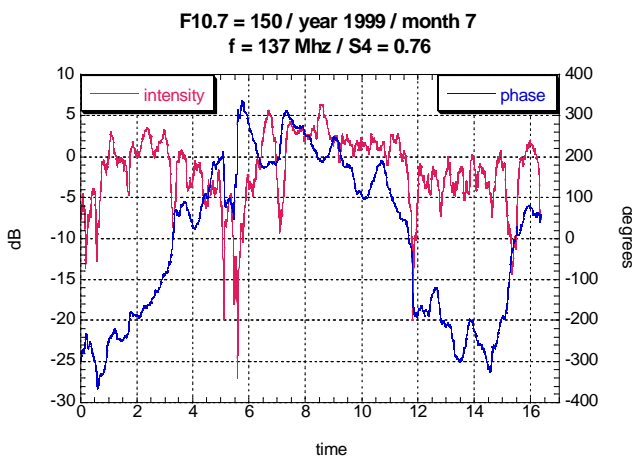
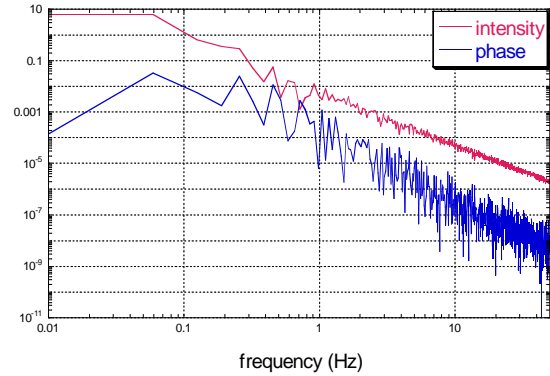


Figure 2 : the spectrum of transmitted signals and a global map

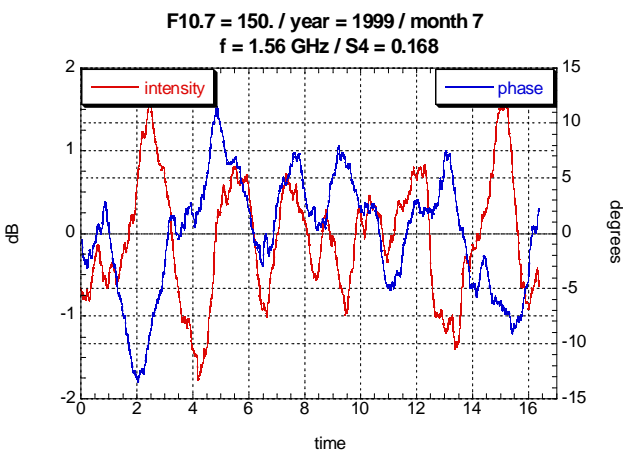


Figure 1 : phase and intensity fluctuations : VHF and L band links

## 3. Scintillations at receiver level

### 3.1 GPS Receiver Architecture

A GPS receiver is a spread spectrum receiver, requiring several essential parts for acquisition, tracking and extracting useful information from the incoming satellite signal. It can be broadly divided into three sections: the RF Front-end (RFF), Digital Signal Processing (DSP) and the Navigation Data Processing (NDP). The RFF and the DSP sections generally consist of various hardware modules, whereas the NDP section is implemented using software. Figure 8 shows a simple block diagram of a typical single frequency GPS receiver with major interfaces and input/output signals of the essential blocks.

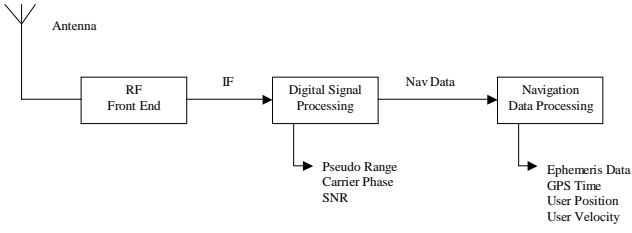


Fig. 3 : Block diagram of a generic GPS receiver

The DSP performs the acquisition and tracking of the GPS signal. Traditional signal demodulation such as those used for FM or AM cannot be used for spread spectrum signals such as GPS because the signal level is below the noise level. Instead, the signal must be coherently integrated over time so that the noise is averaged out, thereby raising the signal above the noise floor.

Any GPS receiver locking onto a GPS satellite signal has to do a two-dimensional search for the signal. The first dimension is time. The GPS signal structure for each satellite consists of a 1023 bit long pseudo-random number (PRN) sequence sent at a rate of 1.023 megabits/sec, i.e. the code repeats every millisecond. To acquire in this dimension, the receiver needs to set an internal clock to the correct one of the 1023 possible time slots by trying all possible values. Once the correct delay is found, it is tracked with a Delay Lock Loop (DLL).

The second dimension is frequency. The receiver must correct for inaccuracies in the apparent doppler frequency. Once the carrier frequency is evaluated, it is tracked with a Phase Lock Loop (PLL). Figure 9 shows an extremely simplified PLL/DLL architecture. A more precise description of the GPS signal processing can be found in [Ward].

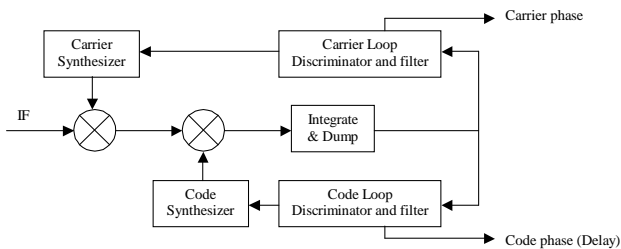


Fig. 4 : Simplified GPS Digital Receiver Channel

### 3.2 Phase Noise at Receiver Level

When the receiver is unable to track the carrier phase, the signal is lost. Loss of lock is directly related with PLL cycle slips. To evaluate the occurrence of cycle slips, the tracking error variance at the output of the PLL has to be considered. This variance is expressed as a sum of three terms [Conker et al]:

$$\sigma_{\phi}^2 = \sigma_{\phi_S}^2 + \sigma_{\phi_T}^2 + \sigma_{\phi_{osc}}^2 \quad (7)$$

where

$\sigma_{\phi_S}$  is the phase scintillation variance,  $\sigma_{\phi_T}$  is the thermal noise variance and  $\sigma_{\phi_{osc}}$  is the receiver oscillator noise (0.122 rad) [Conker et al]. The phase variance scintillation at the output of the PLL is given by [Conker et al] :

$$\sigma_{\phi_S}^2 = \int_{-\infty}^{\infty} |1 - H(f)|^2 S_{\phi}(f) df \quad (8)$$

where  $S_{\phi}(f)$  is the PSD of phase scintillation. Figure 10 shows a phase scintillation spectrum obtained with GISM.  $|1 - H(f)|^2$  is the closed loop transfer function of the PLL and depends on  $k$ , the loop order, and  $f_n$ , the loop natural frequency. Its expression is given by (9). Typical values are  $k = 3$  and  $f_n = 1.91$  Hz.

$$|1 - H(f)|^2 = \frac{f^{2k}}{f^{2k} + f_n^{2k}} \quad (9)$$

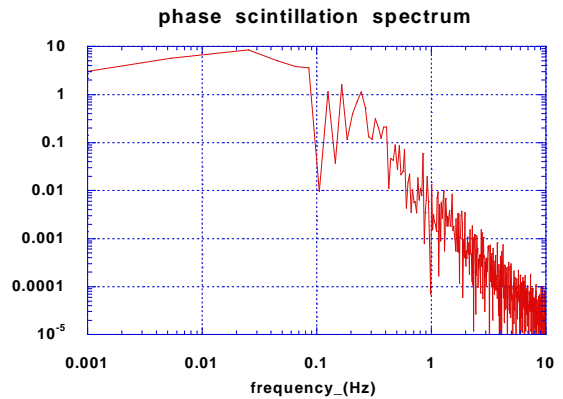


Fig. 5 : PSD of phase scintillation computed with GISM

When there is no scintillation, the standard thermal noise tracking error for the PLL is :

$$\sigma_{\Phi_T}^2 = \frac{B_n}{(c/n_0)} \left[ 1 + \frac{1}{2\eta (c/n_0)} \right] \quad (10)$$

where  $c/n_0$  is the signal to noise ratio (SNR),  $B_n$  is the receiver bandwidth, and  $\eta$  is the predetection time. For airborne GPS receiver,  $B_n = 10$  Hz and  $\eta = 10$  ms. Amplitude scintillation alters the SNR and increases the thermal noise tracking error. According to [Conker et al], in presence of scintillation characterized by  $S_4$  index, thermal noise tracking error is given by :

$$\sigma_{\Phi_T}^2 = \frac{B_n \left[ 1 + \frac{1}{2\eta (c/n_0) (1 - 2s_4^2)} \right]}{(c/n_0) (1 - s_4^2)} \quad (11)$$

Equation (11) needs the evaluation of the SNR. The GPS link budget can be expressed in dB as following :

$$C / N_0 = P_0 + G_t + G_r - \text{Propagation losses} - \text{Insertion Losses} - N_0 \quad (12)$$

where  $P_0$  is the emitted power,  $G_t$  and  $G_r$  are respectively the emitter and the receiver antenna gain, and  $N_0$  is the receiver noise density. Therefore, the SNR appears to be depending on the elevation angle as shown in figure 6.

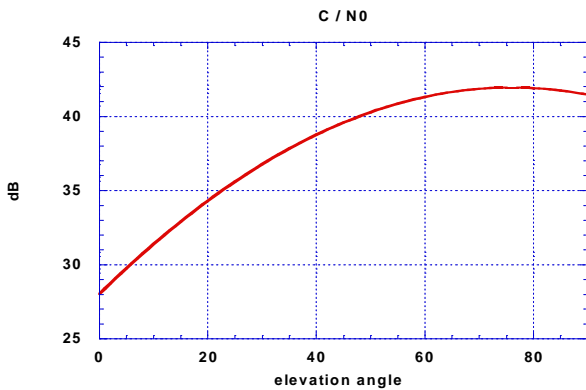


Figure 6 :  $C / N_0$  vs elevation angle without scintillation for a GPS link

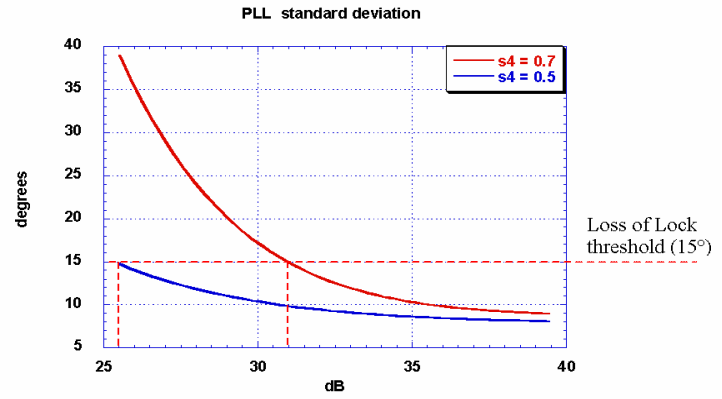


Figure 7 : PLL standard deviation vs  $C / N_0$

Equations (8) and (11) can be used to compute the PLL tracking error variance. Figure 7 is a comparison of this variance vs  $C / N_0$  for  $S_4 = 0.7$  and  $S_4 = 0.5$ . Loss of lock is highly probable for values above the  $15^\circ$  threshold. Therefore a receiver is able to tolerate scintillation if the  $C / N_0$  is above a minimum value. This minimum is 26 dB for  $S_4 = 0.5$  and 32 dB for  $S_4 = 0.7$ .

#### 4. Loss of Lock Probability

Thermal noise appears to be the essential contribution to PLL tracking error. It is the unique  $S_4$  dependent term in (11) and the influence of  $S_4$  is obvious in figure 7. A study of amplitude scintillations is detailed in [Conker et al]. We will present here another approach of amplitude scintillation effects on thermal noise.

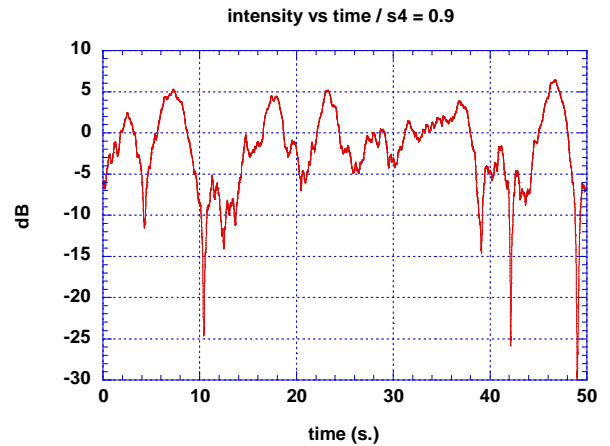


Figure 8 : Scintillation intensity vs time computed with GISM

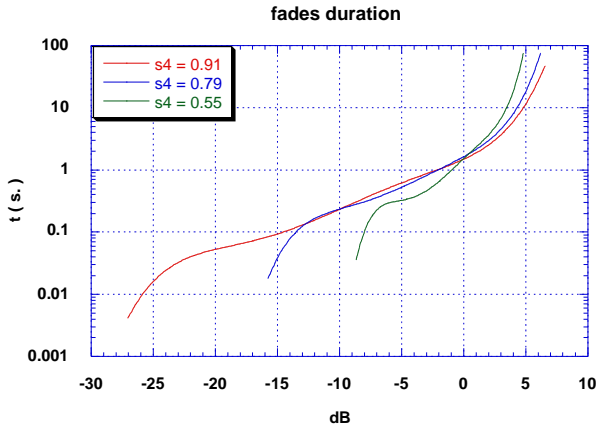


Figure 9 : fades duration vs fade depth

Figure 8 shows a typical signal amplitude under severe scintillation conditions ( $S_4 = 0.9$ ). The corresponding fade duration (figure 9) always exceeds the pre integration duration time. As a consequence it corresponds to a degradation of the SNR at receiver level:

$$c/n = c/n_0 + I_s(\text{in dB}) \tag{13}$$

or, with the fractional form :

$$c/n = c/n_0 * I_s \tag{14}$$

where  $I_s$  is the scintillation intensity. Its mean value is 1 and it has a Nakagami distribution characterized by  $S_4$ .

Equation (11) is modified to take the fading into account :

$$\sigma_{\phi_T}^2 = \frac{B_n}{(c/n_0) I_s} \left[ 1 + \frac{1}{2\eta (c/n_0) I_s} \right] \tag{15}$$

This relation expresses the thermal noise as a decreasing function of the scintillation intensity. As a result, if  $\sigma_{\phi_T}$  is above the  $15^\circ$  threshold then  $I_s$  is below a value computed using (15). As  $I_s$  distribution is known for a given  $S_4$ , the probability of occurrence of " $I_s < \text{threshold}$ " can be evaluated. The result is the probability of Loss of Lock. Figure 10 presents this probability versus  $S_4$  at given values of the SNR. It can be noticed that links with high SNR are quite robust. On the contrary, links with low values of SNR are likely to be lost.

GISM has an integrated GPS satellite trajectory generator. It has been used to simulate a whole day (24th September 2001) over Naha (Japan, latitude =  $26^\circ$  geographic,  $15^\circ$  magnetic). All visible satellites were used to compute an average probability of loss of lock. The result is 0.21 %. In other words, each satellite was 0.21% of the time locked out during that day.

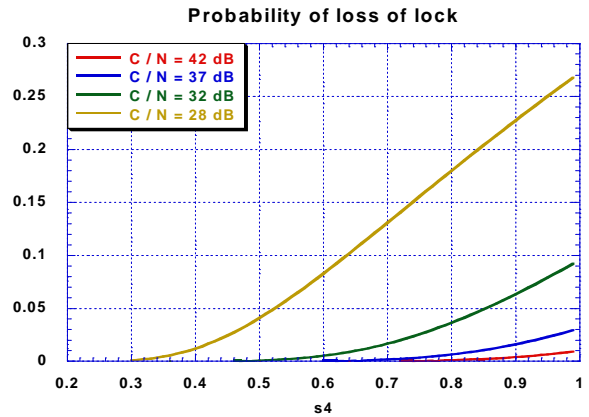


Figure 10 : Probability of loss of lock vs  $s_4$  for 4 values of the SNR

### 5. Positioning Errors

In most cases, scintillations don't affect all visible satellites. If the number of satellites is above 4 then a standard receiver should be able to provide navigation information. However, the number of satellites and their positions affect the positioning precision. The Dilution Of Precision (DOP) is usually used to quantify this precision. The DOP is related to the geometrical distribution of the visible constellation. The DOP is used to derive the positioning error ( $\sigma_p$ ) from the User Equivalent Range Error (UERE):

$$\sigma_p = \text{DOP} * \text{UERE} \tag{16}$$

GISM was used to compute all scintillation parameters for each GPS satellite visible from Naha (Japan). The tracking error was derived from these parameters and from typical receiver characteristics. Satellites with tracking error above the  $15^\circ$  threshold were ignored for the DOP evaluation.

Even if the signal emitted from a GPS satellite isn't lost, it can alter the position precision. One

of the DLL functions is the measurement of the delay between the code carried by the GPS signal and the receiver internal clock. This delay is an estimation of the time needed by the GPS signal to reach the receiver. The receiver is then able to compute the distance of the satellite. Errors in this estimation are collected in the UERE. To take the scintillations into account, we have to consider the DLL tracking errors.

The DLL can be studied like the PLL to evaluate its tracking error variance in degrees. The UERE due to scintillations can then be deduced with a product with the chip length (equal to 293 m for L1). The results are shown in Figure 11. These results seem to show high degradation of the UERE. Satellites with high DLL tracking errors have also high PLL tracking errors and therefore they might be considered as lost and don't contribute to the UERE.

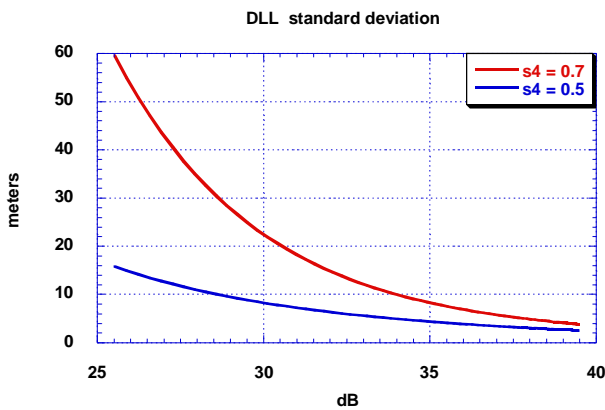


Figure 12: DLL tracking error vs C/N0

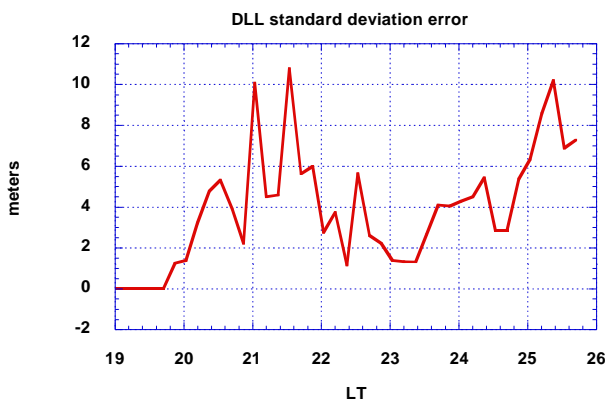


Figure 13 : Positioning error at Naha (Japan) under scintillation conditions, computed with GISM

The combination of both effects is presented in Figure 12. Satellites with PLL tracking errors above  $15^\circ$  were considered invisible for the DOP calculation. All other links with visible satellites

were used to compute a mean UERE contribution due to scintillation.

## 6 Hybrid simulation with GISM and GSS SPIRENT Simulator

### 6.1 Statement of the problem

LRBA (the Ballistic and Aerodynamic Research Laboratory) is the DGA technical center (French Military Defence Administration) for all the military applications using the information coming from Global Navigation Satellite Systems as GPS or GLONASS. One of the main issues in the link budget error analysis (the User Equivalent Range Error (UERE)), is the ionosphere which induces errors different for the code and the phase as explained in the previous sections.

GISM simulator allows estimating the effects of the ionosphere on the transmitted signals both at receiver level and including that one with specific characteristics. In this study we have included GISM in a more global software allowing synthesizing the signal and checking consequently some of the results previously presented. The work, still on-going, combines GISM results with a radiofrequency signal generator : the GSS SPIRENT 4760. It allows generating different GNSS channel characteristics in order to test real receivers in the laboratory. New functions have been added on this signal simulator as for example a multipath function capability.

GISM simulation results are used in the hybrid test bed to increase the degree of representativity of the laboratory tests. Several technical difficulties have been encountered during this project, in particular for the choice of the methodology to be used to package GISM outputs with GSS SPIRENT inputs.

## 6.2 The GSS Simulator SPIRENT 4760

The GSS Simulator SPIRENT allows generating totally different GNSS signal channels via a control station allowing defining the parameters of the space segment, the channel modelling and the user segment.

## 6.3 Scintillation simulation

GISM software has been included in the simulator test equipment in conjunction with GPS signals generators (SPIRENT 4760) to evaluate the effect of the scintillations on the received signals. These generators have “a user defined” mode allowing including errors set by the user. This mode has been used for this study.

Taking scintillations into account is done in two steps:

In a first step we evaluate the amplitude and phase standard deviations ( $S_4$  and  $\sigma_\phi$ ). This

calculation is performed every 3 minutes because this duration can be considered as well below the time correlation of  $S_4$  and  $\sigma_\phi$ . Below this duration the scintillations are considered as a stationary process.

In a second step, we generate a scintillation like signal i.e. the corresponding intensity and phase. Both are random variables. The spectrum exhibits a power law variation in both cases. It is also an output of GISM. The related probabilities correspond to an m-Nakagami law for the intensity, with  $m = 1/S_4^{*2}$  ant to a Gaussian law for the phase with zero as mean value and  $\sigma_\phi$  as a standard deviation. The values of the intensity and phase are obtained using a random generator which synthesizes a signal with these properties at a sampling frequency chosen by the user. This frequency is set to 1 Hz.

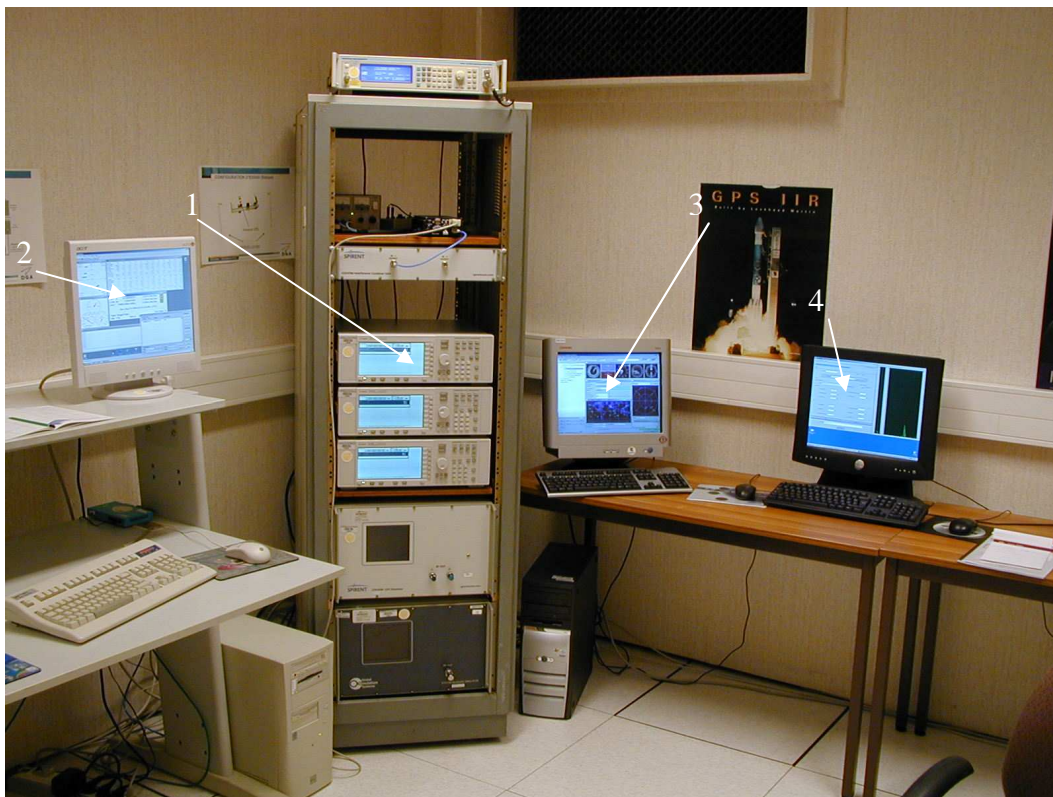


Figure 14 : Experimental set up

Receiver under test (Novatel OEM3) (1); Receiver input unit (2); Spirent GPS constellation generator (3); Spirent simulator command unit (4) ; GISM simulator (5)



As regards the effects on the receiver, the phase is an additional noise in the phase loop and the intensity, considering its time duration, is added to the signal. It corresponds consequently to a decrease of the signal to noise ratio. This being done, we obtain more realistic ionosphere errors allowing to assess bi-frequency L1-L2 receivers as well as differential correcting systems.

### Results obtained

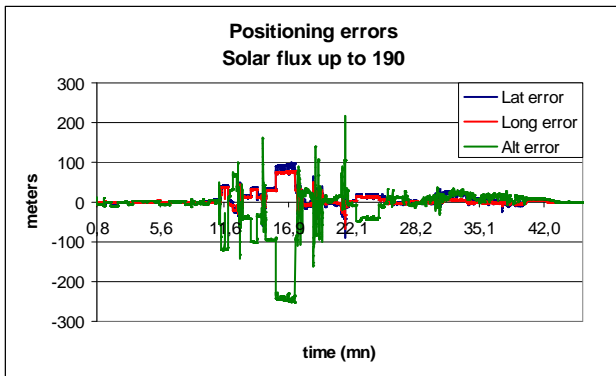


Figure 15: Positioning error vs GPS time

Preliminary results have been obtained and are presented on figure 15 for the positioning errors in latitude, altitude and longitude. The solar flux was varying between 100 and 190 in this simulation. The scintillations module was activated in the simulator at  $t = 10$  mn and deactivated at  $t = 40$  mn. Positioning errors reach 200 meters in the worst case. The vertical error is greater than the horizontal error as expected.

### 7. Conclusion

The scintillations characteristics and their effect on receivers have been presented. A random signal generator has been developed allowing including this effect in a more global GPS receiver simulator in order to assess what has been estimated in the theoretical analysis.

Preliminary results have been obtained. Present work is dedicated to the homogenisation and the consolidation of the procedure for using GISM results in the hybrid test bed. The DLL, the positioning errors and the probabilities of loss of lock will then be estimated varying the

geophysical conditions for a few observations points at the equator and at auroral regions.

### 8. References

M.B. El Arini, R. Conker, Y. Béniguel, J-P Adam, "Comparing measured s4 with the calculated s4 by the WBMOD and GISM at Naha, Japan", SBAS meeting, Portland, Oregon, september 2003

Y. Béniguel "Global Ionospheric Propagation Model (GIM): A propagation model for Scintillations of Transmitted Signals", Radio Science, Mai-juin 2002

Y. Béniguel, J-P Adam, J. Geiswiller, "Characterisation of Ionosphere Scintillations PLL and DLL Errors at receiver level", *Proc. of the Atmos. Remote Sensing Conference*, Matera (Italy) 2003, URSI, 2003.

Conker, R. S., M. B. El-Arini, C. J. Hegarty, T. Hsiao, "Modeling the Effects of Ionospheric Scintillation on GPS/SBAS Availability", *Radio Science*, January/February 2003.

P. Doherty, S. Delay, C. Valladares "Ionospheric Scintillations Effects in the Equatorial and Polar Regions" ION GPS Symposium, Salt Lake City (UT) 2000.

K. Matsunaga "Observation of Ionospheric Scintillations on GPS Signals in Japan", ION symposium, 2002

P. Ward, "Satellite Signal Acquisition and Tracking", *Understanding GPS Principles and Applications*, ed. E.D. Kaplan, Artech House, Boston, pp. 119-208, 1996.

Y. Béniguel, B. Forte, S. Radicella, H. Strangeways, V. Gherm, and N. Zernov, "Scintillations effects on earth terrestrial links for telecommunication and navigation purposes", *Annals of Geophysics*, Vol 47, 2004